Electron energy distribution function, plasma potential and electron density measured by Langmuir probe in tokamak edge plasma

2009 Plasma Phys. Control. Fusion 51 065014

(http://iopscience.iop.org/0741-3335/51/6/065014)

IOP PUBLISHING PLASMA PHYSICS AND CONTROLLED FUSION

Plasma Phys. Control. Fusion **51** (2009) 065014 (15pp) doi:10.1088/0741-3335/51/6/065014

Electron energy distribution function, plasma potential and electron density measured by Langmuir probe in tokamak edge plasma

Tsv K Popov[1], P Ivanova[1], J Stöckel[2] and R Dejarnac[2]

[1] Faculty of Physics, St Kliment Ohridski University of Sofia, 5 J. Bourchier Blvd., 1164 Sofia, Bulgaria
[2] Institute of Plasma Physics, Academy of Sciences of the Czech Republic v.v.i., Za Slovankou 3, 182 00 Prague 8, Czech Republic

E-mail: tpopov@phys.uni-sofia.bg

Received 2 December 2008, in final form 10 March 2009
Published 29 April 2009
Online at stacks.iop.org/PPCF/51/065014

Abstract

The electron energy distribution function (EEDF) at different radial positions is derived from Langmuir probe measurements in the CASTOR tokamak edge plasma using the first derivative method. It is shown that the EEDFs are not Maxwellian but can be approximated as bi-Maxwellians with one dominant, low temperature electron population and one minority composed of hotter electrons. In the limiter shadow the measured EEDFs are Maxwellian. The values of the plasma potential and electron densities at different radial positions are also evaluated. The results presented in this paper demonstrate that the first derivative method allows one to acquire additional plasma parameters using the electron part of the current–voltage characteristics in strongly magnetized tokamak edge plasmas.

(Some figures in this article are in colour only in the electronic version)

1. Introduction

Among the contact methods of plasma diagnostics, the electric probes are the most reliable diagnostic tools allowing one to measure edge plasma parameters with sufficiently high temporal and spatial resolution. In non-magnetized, low density plasmas Langmuir probes (LPs) allow local measurements of the plasma potential, the charged particles density and the electron energy distribution functions (EEDFs), $f(\varepsilon)$ [1–7].

In magnetized plasma, the interpretation of the electron part of the current–voltage (IV) characteristics above the floating potential, U_{fl}, remains till now problematic—the electron part of the IV characteristics is distorted due to the influence of the magnetic field. For this reason, in the strongly magnetized tokamak plasmas the ion saturation branch of the

I V and the part around the floating potential are usually used when retrieving the plasma parameters [8, 9]. This method assumes a Maxwellian EDF for the electrons and could lead to erroneous values if it is not the case. In tokamaks, this assumption is generally valid. However, some experimental evidence of non-Maxwellian distributions in tokamak edge plasmas is confirmed. In ASDEX, the electron temperatures measured by a LP, assuming a Maxwellian EEDF, are about twice as high as that determined from Thomson scattering [10]. Under some circumstances [11, 12] the EEDF may be approximated as a two-temperature (bi-Maxwellian) distribution with a dominant electron population of low temperature and a minority of electrons with high temperature. In the Stangeby paper [11] the reasons for the presence of a minority fraction of electrons with high temperature are widely discussed as well as the problems in the interpretation of the *I V* characteristics for evaluating the electron temperatures. The presence of a small population of suprathermal electrons can also contribute to the discrepancy between LP and tunnel probe electron temperatures measurements [13–15] in CASTOR tokamak edge plasma.

The knowledge of the real EEDF is of great importance in understanding the underlying physics of processes occurring at the plasma edge in tokamaks, such as the formation of transport barriers, plasma–wall interactions, and edge plasma turbulence. The kinetic theory developed in the non-local approach [6, 16, 17] may be used for the evaluation of the EEDF from the first derivative of the electron current of the *I V* characteristics. In this work we report the EEDFs measured by LPs at different radial positions in the CASTOR tokamak using this technique, and the values of the plasma potential, the electron temperatures and densities are presented.

2. First derivative LP method

A kinetic theory for processing the electron probe current in the presence of a magnetic field was published in [17]. The theory for magnetized plasmas was developed for LPs in a non-local approach when the electrons reach the probe in the diffusion regime. The tokamak plasma is considered usually as non collisional plasma. The edge plasma is strongly turbulent plasma. In the turbulence the vector of the electric field changes its orientation in arbitrary directions. This causes changes in the direction of the electrons motion but does not change their kinetic energy. The result is similar to elastic collisions [18] and for turbulent edge plasma we can use the method for evaluating the EEDF presented in [17]. It is shown that the electron current flowing to a cylindrical probe, negatively biased by potential U_p, is given by

$$I_\mathrm{e}(U) = -\frac{8\pi eS}{3m^2}\int_{eU}^{\infty}\frac{(W-eU)f(W)\,\mathrm{d}W}{\gamma(W)\left[1+\dfrac{(W-eU)}{W}\psi(W)\right]}, \tag{1}$$

where W is the electron energy, e, m and n are the electron charge, mass and density, S is the probe area, U is the probe potential with respect to the plasma potential U_pl ($U = U_\mathrm{p} - U_\mathrm{pl}$). The geometric factor $\gamma = \gamma(R/\lambda)$ assumes values in the range $0.71 \leqslant \gamma \leqslant 4/3$ (R being the probe radius) [17].

Here $f(W)$ is the isotropic EEDF, normalized by

$$\frac{4\pi\sqrt{2}}{m^{3/2}}\int_0^{\infty} f(W)\sqrt{W}\,\mathrm{d}W = \int_0^{\infty} f(\varepsilon)\sqrt{\varepsilon}\,\mathrm{d}\varepsilon = n \tag{2}$$

and the diffusion parameter $\psi(W)$ is given by

$$\psi(W) = \frac{1}{\gamma\lambda(W)}\int_R^{\infty}\frac{D(W)\,\mathrm{d}r}{(r/R)D(W-e\phi(r))}. \tag{3}$$

Here $D = v\lambda(W)/3$ is the diffusion coefficient, where $\lambda(W)$ is the free path of the electrons with velocity v and energy W. $\phi(r)$ is the potential variation introduced by the probe.

Let us consider the boundary cases regarding the value of the diffusion parameter:

(1) When $\psi(W)$ is negligible ($\psi \ll 1$) and $\gamma = 4/3$, equation (1) is reduced to the classical expression of the Langmuir formula for the electron probe current:

$$I_e(U) = -\frac{2\pi eS}{m^2}\int_{eU}^{\infty}(W - eU)f(W)\,\mathrm{d}W. \tag{4}$$

This approximation is valid at low gas pressure or for low magnetic fields; namely when the electron free path or the Larmor radius are larger than the characteristic dimension of the probe sheath. Then the EEDF can be determined by using the Druyvesteyn formula [1]:

$$f(\varepsilon) = \frac{2\sqrt{2m}}{e^3 S}\frac{\mathrm{d}^2 I_e}{\mathrm{d}U^2}. \tag{5}$$

(2) At strong magnetic fields or namely for high values of the diffusion parameter ($\psi \gg 1$), it has been shown [6, 17] that the EEDF is not represented by the second derivative of the electron probe current (Druyvesteyn formula) but rather by its first derivative.

Obviously to evaluate the EEDF the values of the diffusion parameter have to be known. In the presence of a magnetic field, ψ depends on the plasma parameters, the shape, the size and the orientation of the probe with respect to the magnetic field.

Let us consider a cylindrical LP with the radius R and the length L, oriented perpendicularly with respect to the magnetic field in tokamak edge turbulent plasma. We can write the diffusion parameter $\psi_\perp$ as follows:

$$\psi_\perp(W) = \frac{1}{\gamma\lambda(W)}\int_R^A \frac{D(W)\,\mathrm{d}r}{(r/R)D(W - e\phi(r))}. \tag{6}$$

In equation (3) the upper limit is $A = \infty$ and the integral is divergent, therefore we have to find a reasonable finite value for A. In non-magnetized plasma the probe disturbed area is taken as a prolate ellipsoid of revolution [6, 17] and the integral is limited to the value of $A = \pi L/4$. In homogeneous magnetized plasma the upper limit of the integral has to be enlarged up to the value of $A = \pi\rho L/4$ [17], with ρ defined by

$$\rho = \left[1 + \frac{\lambda(W)^2}{R_L(W, B)^2}\right]^{1/2}. \tag{7}$$

For magnetic fields B in the range 1–5 T the electron Larmor radius $R_\mathrm{L}(W, B) \ll \lambda(W)$. Then we have

$$\rho = \left[1 + \frac{\lambda(W)^2}{R_\mathrm{L}(W, B)^2}\right]^{1/2} \approx \frac{\lambda(W)}{R_\mathrm{L}(W, B)}. \tag{8}$$

The value of ρL may exceed one toroidal turn in the tokamak chamber. On the other hand, in turbulent plasma the probe disturbed area may be limited to the characteristic size of the turbulence L', which is typically in the order of 0.01 m in CASTOR [19], and therefore we replace ρL in the upper limit of the integral by L' and we write (6) as

$$\psi_\perp(W) = \frac{1}{\gamma\lambda(W)}\int_R^{\frac{\pi L'}{4}} \frac{D(W)\,\mathrm{d}r}{(r/R)D(W - e\phi(r))}. \tag{9}$$

The second important point is the ratio of the coefficients of the global diffusion $D(W)$ over diffusion in the vicinity of the probe $D(W - e\phi(r))$. In turbulent plasma the global diffusion is given by the Bohm diffusion and therefore we can write [18, 20]

$$\frac{D(W)}{D(W - e\phi(r))} = \frac{D_\mathrm{Bohm}}{D} = \frac{1}{16}\frac{\lambda(W)}{R_L(W, B)} \approx \frac{\rho}{16}. \tag{10}$$

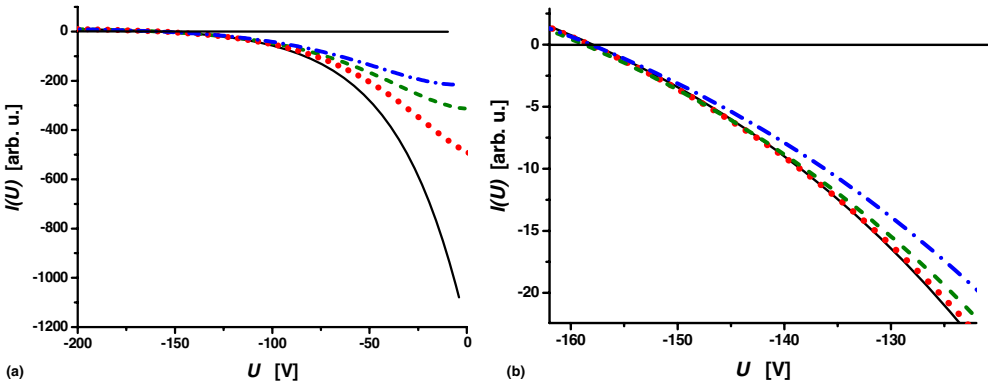

Figure 1. (*a*) Plots of model calculations of the probe current at electron temperature $T = 35$ eV and at different ψ_0: solid line—$\psi_0 = 0$ (no magnetic field), dots—$\psi_0 = 25$, dashed line—$\psi_0 = 50$ and dash–dot line—$\psi_0 = 75$. (*b*) Zoom-in of figure 1(*a*)) curves in the area of floating potential and cutoff potential. In the figures the plasma potential $U_{\rm pl}$ is set at 0.

Then we can write for the diffusion parameter:

$$\psi_\perp(W) = \frac{1}{\gamma\lambda(W)} \int_R^{\frac{\pi L'}{4}} \frac{\rho\, \mathrm{d}r}{16(r/R)}$$

and finally we have

$$\psi_\perp(W) = \frac{R \ln\left(\dfrac{\pi L'}{4R}\right)}{16\gamma R_L(W, B)}. \tag{11}$$

For probes oriented parallel with respect to the magnetic field, the probe disturbed area is taken as an oblate ellipsoid of revolution [17] and the diffusion parameter can be written as

$$\psi_\parallel(W) = \frac{\pi L'}{64\gamma R_{\rm L}(W, B)}. \tag{12}$$

Similar expressions for the diffusion parameters (11) and (12) but for non-turbulent plasmas are obtained in [21, 22].

In the papers [6, 17, 23] ψ is only considered a constant. As it is seen from (11) and (12) in the presence of a magnetic field the diffusion parameter depends on the electron energy: $\psi(W) = \psi_0/\sqrt{W}$, where ψ_0 is a part of the diffusion parameter which is constant with regard to the electron energy. The typical values of ψ_0 for a cylindrical probe with a radius $R = 1$ mm and a length $L = 2$–3 mm, a magnetic field $B = 1.5$ T and a characteristic size of the turbulence $L' \sim 1$ cm are in the order of 50 for a perpendicular oriented to the magnetic field probe and 150–200 for a parallel oriented one.

From equation (1) it is seen that as the value of the diffusion parameter increases, so does the distortion of the electron probe current. Figure 1 presents model calculations of the probe current at different values of the diffusion parameter.

As is seen in figure 1(*b*), as the value of the diffusion parameter is increased, the value of the cutoff voltage $U_{\rm c}$ where the curve starts to deviate from the exponential behaviour is shifted towards the floating potential $U_{\rm fl}$. In figure 1 $U_{\rm fl} = -158$ V. For $\psi_0 = 25$ the cutoff voltage $U_{\rm c} = -130$ V, for $\psi_0 = 50$ it is $U_{\rm c} = -140$ V and for $\psi_0 = 75$ it is $U_{\rm c} = -150$ V. For a probe oriented perpendicularly to the magnetic field, the value of the diffusion parameter is proportional to the probe radius (equation (11)) and, thus, increasing the

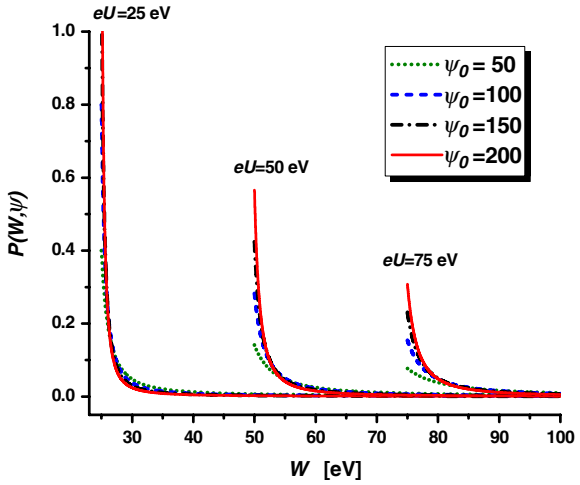

Figure 2. Plots of the function $P(W, \psi)$ at different ψ_0 and different values of eU.

probe radius leads to the value of the cutoff voltage U_c approaching the floating potential U_{fl}. This was experimentally observed by Hidalgo *et al* [24].

The values of the diffusion parameter having been evaluated, we can consider the first derivative probe method for obtaining the EEDF. The first derivative of the electron probe current (equation (1)) is

$$I'_e(U) = \frac{dI_e(U)}{dU} = -\text{const} \int_{eU}^{\infty} K'(W, U) f(W)\, dW, \tag{13}$$

where $K'(W, U) = \frac{W^2}{[W(1+\psi)-\psi eU]^2}$.

One can write $K'(W, U)$ as a sum of two terms $K'_1(W, U)$ and $K'_2(W, U)$ as follows:

$$K'(W, U) = \frac{\psi eU W}{(1+\psi)[eU + (1+\psi)(W - eU)]^2} + \frac{W}{(1+\psi)[eU + (1+\psi)(W - eU)]}. \tag{14}$$

Then for the integral of the first term we can write

$$I'_{e1}(U) = -\text{const} \int_{eU}^{\infty} \frac{eU}{1 + \frac{\psi_0}{\sqrt{W}}} \frac{\frac{\psi_0}{\sqrt{W}} f(W)\, dW}{W \left[1 + \frac{\psi_0}{\sqrt{W}} \left(1 - \frac{eU}{W}\right)\right]^2}$$

$$= -\text{const} \int_{eU}^{\infty} \frac{eU}{1 + \frac{\psi_0}{\sqrt{W}}} P(W, \psi) f(W)\, dW. \tag{15}$$

The plots of the function $P(W, \psi)$ at different ψ_0 and different values of eU are presented in figure 2. The curves have a sharp maximum and the integral $\int_{eU}^{\infty} P(W, \psi)\, dW \approx 1$ with accuracy between 4% to 15%.

Due to its behaviour the function $P(W, \psi)$ may be replaced by $P(W, \psi) \underset{\psi_0 \gg 1}{\longrightarrow} \delta_+(W - eU)$ and the integration performed:

$$I'_{e1}(U) = -\text{const} \int_{eU}^{\infty} \frac{eU}{1 + \frac{\psi_0}{\sqrt{W}}} \delta(W - eU) f(W)\, dW = -\text{const} \frac{eU}{1 + \frac{\psi_0}{\sqrt{eU}}} f(eU).$$

At $\psi(W) \gg 1$ we obtain

$$I'_{e1}(U) = -\text{const}\frac{eU}{\frac{\psi_0}{\sqrt{eU}}} f(eU) = -\text{const}\frac{eU\sqrt{eU}}{\psi_0} f(eU). \tag{16}$$

The second term of the integral (13) is

$$I'_{e2}(U) = -\text{const}\int_{eU}^{\infty} \frac{W f(W)\,\mathrm{d}W}{\left(1+\frac{\psi_0}{\sqrt{W}}\right)\left[\left(1+\frac{\psi_0}{\sqrt{W}}\right)W - \frac{\psi_0}{\sqrt{W}}eU\right]} \tag{17}$$

and combining (16) and (17) we obtain for the first derivative of the electron probe current

$$I'_e(U) = -\text{const}\frac{eU\sqrt{eU}}{\psi_0} f(eU) - \text{const}\int_{eU}^{\infty} \frac{W f(W)\,\mathrm{d}W}{\left(1+\frac{\psi_0}{\sqrt{W}}\right)\left[\left(1+\frac{\psi_0}{\sqrt{W}}\right)W - \frac{\psi_0}{\sqrt{W}}eU\right]}. \tag{18}$$

In the case of high gas-pressure plasmas [6, 17] (constant ψ) or in magnetized plasma [21, 22] ($\psi = \psi(W)$) the contribution of the second term was always assumed small and therefore neglected. Then the EEDF is directly represented by the first derivative of the electron probe current. In our opinion, the neglect of the second term in strongly magnetized tokamak edge plasma measurements has to be reconsidered. For this purpose, model calculations of the first derivative probe current for a Maxwellian EEDF at $T = 10\,\text{eV}$ and for different values of the diffusion parameter are carried out and shown in figure 3.

One can see from figure 3 that the slopes of the solid lines and the dash–doted lines are identical. Moreover the slopes of the solid lines and the dashed lines differ and the difference increases with the decrease in the diffusion parameter. This behaviour will cause errors in evaluating the electron temperature for values of the diffusion parameter lower than 100 using only the first term (equation (16)). The difference in the position of the minimum of the first derivatives, which is important for evaluating the plasma potential [25], also increases with a decrease in the diffusion parameter. The area of the curves, which is proportional to the electron densities, differs for $\psi_0 > 100$ in the range 2–5%.

In summary, we assume that we can evaluate the EEDF with sufficient accuracy for $\psi_0 > 100$ using only the first term of equation (18) as follows:

$$j'_e(U) = -\text{const}\frac{eU\sqrt{eU}}{\psi_0} f(eU). \tag{19}$$

Taking into account equation (11) for the EEDF measured by a cylindrical probe perpendicular to the magnetic field we obtain

$$f(\varepsilon) = -\frac{3\sqrt{2m}R\ln\left(\frac{\pi L'}{4R}\right)}{32e^3 S R_L(\varepsilon, B)U}\frac{\mathrm{d}I}{\mathrm{d}U}. \tag{20}$$

The EEDF measured by a cylindrical probe parallel to the magnetic field is expressed as

$$f(\varepsilon) = -\frac{3\pi\sqrt{2m}L'}{128e^3 S R_L(\varepsilon, B)U}\frac{\mathrm{d}I}{\mathrm{d}U}. \tag{21}$$

When $\psi_0 < 100$, we have to use an iterative procedure according to equation (18) to obtain the EEDF.

Finally, for acquiring the EEDF one has to know the plasma potential U_{pl}. When the diffusion parameter $\psi(W)$ is negligible ($\psi \ll 1$) the electron probe current is described by

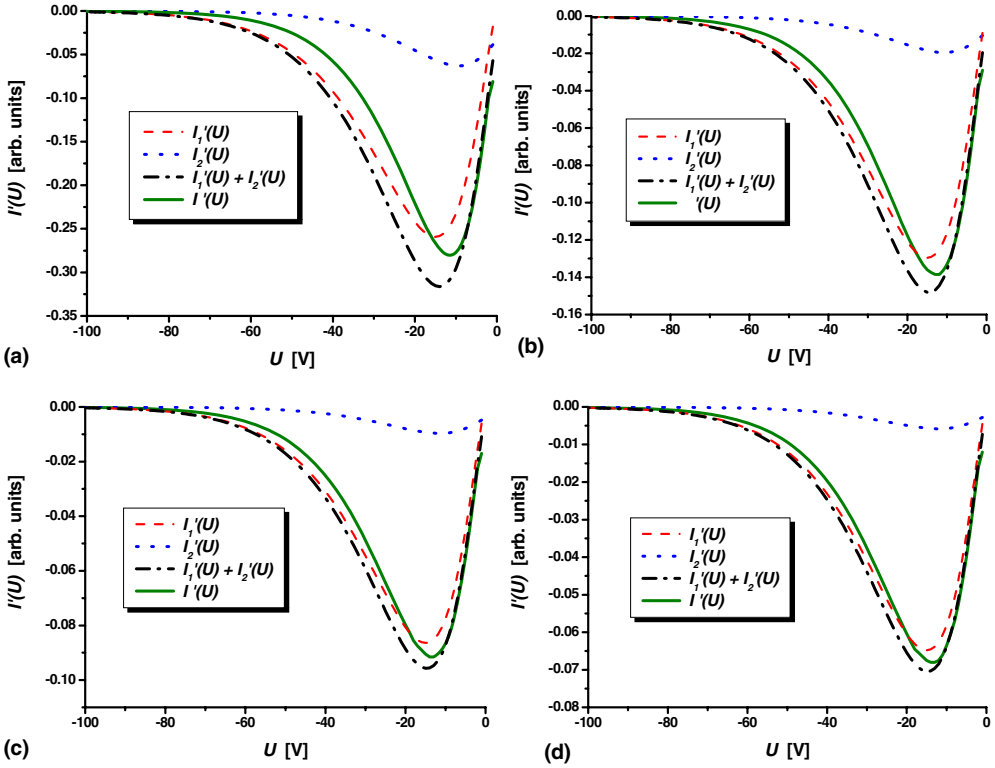

Figure 3. Model calculations of the first derivative probe current for Maxwellian EEDF at $T = 10$ eV. With dashed line the first term of equation (18) is presented, with dots—the second term and with dash–dot—the sum. For comparison with the solid line the first derivative of the probe current (equation (1)) is presented for different values of the diffusion parameter: (*a*) $\psi_0 = 50$; (*b*) $\psi_0 = 100$; (*c*) $\psi_0 = 150$ and (*d*) $\psi_0 = 200$.

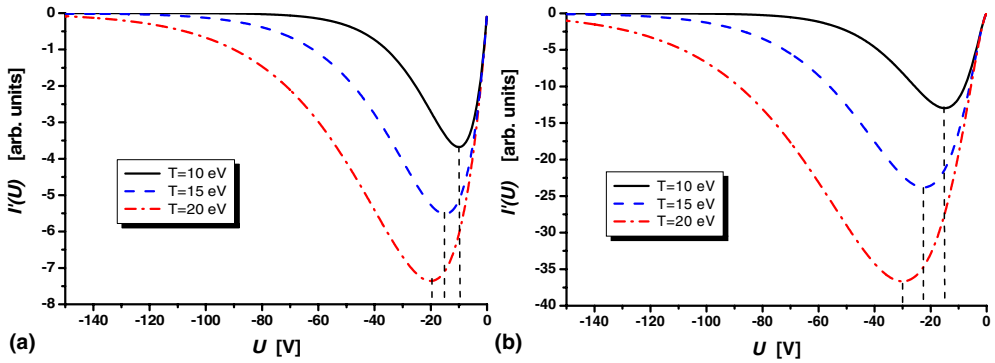

Figure 4. Model calculations of the first derivative of the IV characteristics at (*a*) constant $\psi \gg 1$ and (*b*) $\psi(W) = \psi_0/\sqrt{W} \gg 1$.

equation (4) and the plasma potential is estimated at the position of the bend of IV characteristic or at the minimum of its first derivative. As shown in [6], for a large, constant value of the diffusion parameter $\psi = \psi_0 \gg 1$, the minimum of the first derivative of the IV characteristic is shifted towards negative probe potentials with respect to the plasma potential (set at 0 in figure 4) by a value equal to the electron temperature T expressed in volts (figure 4(*a*)).

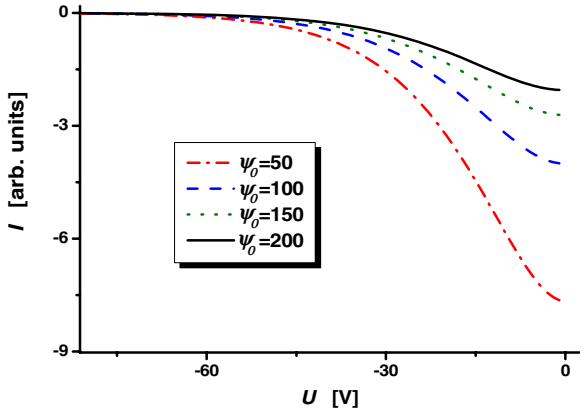

Figure 5. Model calculations for a Maxwellian EEDF ($T = 10$ eV) of the IV characteristics (equation (1)) at different values of ψ_0 in the diffusion parameter $\psi(W) = \psi_0/\sqrt{W}$.

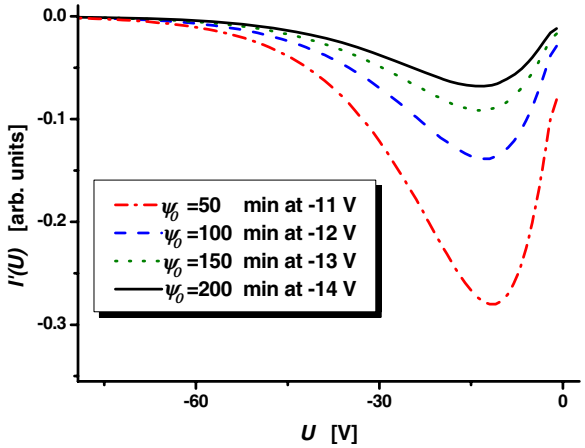

Figure 6. Model calculations for a Maxwellian EEDF ($T = 10$ eV) of the first derivative of the IV characteristics at different values of ψ_0 in the diffusion parameter equation $\psi(W) = \psi_0/\sqrt{W}$.

In the presence of a strong magnetic field the diffusion parameter is large but not constant $\psi(W) = \psi_0/\sqrt{W}$. In the case of $\psi(W) \gg 1$, our model calculations [25] for a Maxwellian EEDFs with different electron temperatures (figure 4(*b*)) show that the minimum is shifted by a value equal to $1.5\,T$.

In the case of intermediate $\psi(W) = \psi_0/\sqrt{W} > 1$ the minimum of the first derivative of the IV characteristic is shifted negatively by a value between T and $1.5\,T$ with respect to the plasma potential. The model calculations for a Maxwellian EEDF ($T = 10$ eV) of the electron probe current using equation (1) are presented in figure 5. Figure 6 shows its first derivatives for different values of ψ_0.

In this case, for an accurate evaluation of $U_{\rm pl}$, we propose the following procedure: the electron temperature is evaluated from the slope in logarithmic scale of the first derivative of the experimental IV characteristic. Using this temperature a model curve of the first derivative (derivative of equation (1)) is calculated. Then the best fit with the experimental first derivative provides the value of the plasma potential.

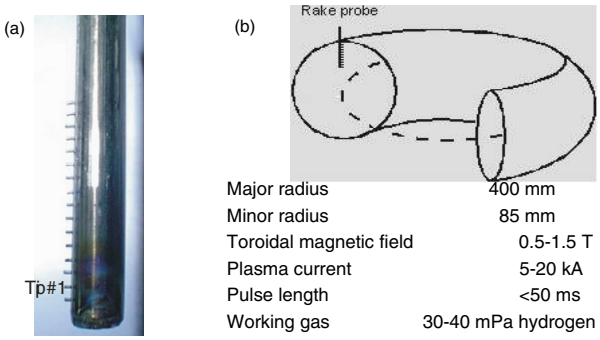

Figure 7. (*a*) Photograph of the rake probe; (*b*) the main parameters of the CASTOR tokamak are listed and the schematic position of the rake probe is presented.

3. LP measurements in CASTOR tokamak edge plasma

For evaluating the EEDF the IV characteristics were measured by using two arrays of cylindrical LP tips (rake probe) with a length L of 2 mm and a radius of 0.35 mm The first rake probe (figure 7) consists of 16 tips oriented perpendicular to the magnetic field lines and the second one of 12 probes oriented parallel to the magnetic field lines. One rake probe was inserted at a time in the edge plasma from the top of the tokamak. The tips are displaced radially by 2.5 mm from each other covering a range of about 40 mm in the plasma. All probe tips are biased simultaneously by a triangular voltage $U_{\mathrm{p}}(t)$ with respect to the tokamak chamber wall, which serves as a reference electrode with a temporal resolution of 1 μs. The time necessary to measure a single IV characteristic is typically $\sim$1 ms.

The measurements were carried out at the CASTOR tokamak edge plasma in two reproducible discharges corresponding to probes oriented perpendicular and parallel to the magnetic field, respectively. The main plasma parameters of these two discharges are presented in figure 8. The magnetic field was 1.3 T. Measurements were performed on the steady-state part of the discharge at low loop voltage, high density, constant plasma current and with low recycling at the chamber.

The data corresponding to the deepest probe of shot # 26402 with perpendicular orientation and located at 56 mm from the centre of the CASTOR poloidal cross-section are presented in figure 9.

To demonstrate the procedure [25] of evaluating U_{pl}, $f(\varepsilon)$ and n, we will analyse a single IV characteristic on the steady-state phase of the plasma current ($10 < t < 11$ ms) as seen from figure 8. The single IV characteristic (1024 points) was smoothed by adjacent averaging of 100 points (figure 10).

Figure 11 presents the first derivative of the smoothed IV curve. In the same figure the fit with the model curve (first derivative of equation (1)) is presented. From comparison the plasma potential $U_{\mathrm{pl}} = 61$ V may be evaluated. One can observe there a more or less pronounced bend in the experimental curve. In practice, even a small increment of $I(U)$ at a probe potential U positive with respect to plasma potential leads to $I'(U)$ deviating from zero at U_{pl}. Additional reasons for this feature come from the plasma potential fluctuations due to the plasma turbulence and the smoothing of the experimental IV characteristic.

In figure 12(*a*) the EEDF obtained for perpendicular probe #1, shot #26402, by using equation (18) (black curve) is presented. It is clearly seen that the EEDF is non-Maxwellian. The EEDF may be approximated by a bi-Maxwellian with low temperature (dash line;

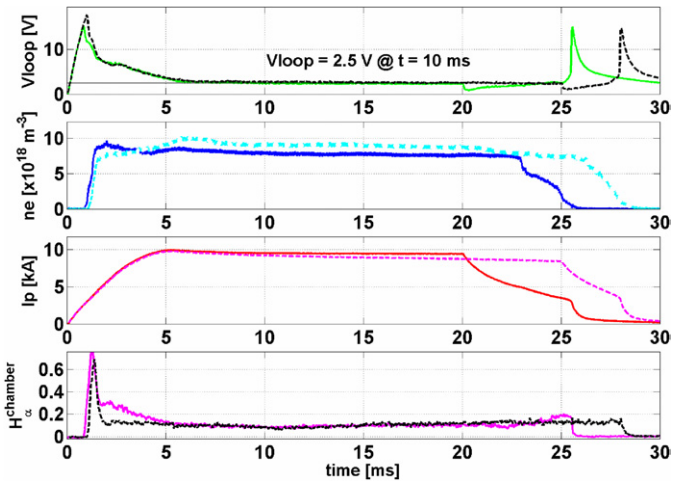

Figure 8. Main plasma parameters of two reproducible discharges: Shot 26402 (solid line) and shot 27034 (dashed line).

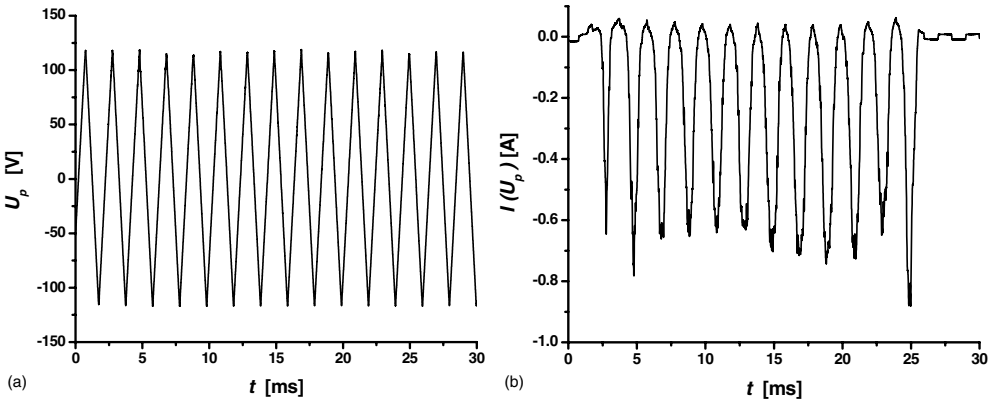

Figure 9. (*a*) Probe bias U_p and (*b*) probe current $I\,(U_p)$ as a function of time t during shot #26402 for perpendicular probe #1 (the deepest), displaced by 56 mm from the centre of the tokamak poloidal cross-section.

$T = 17$ eV) electron fraction and one with high temperature (dot line; $T = 35$ eV). The dash–dot line is a sum of the dotted line and the dashed line. The electron densities are obtained by using equation (2). The density of the high electron temperature fraction is 16% of the cold ones. Similar results from shot #27034 are obtained by using equation (21) for probes oriented parallel to the magnetic field (figure 12(*b*)).

4. Results and discussion

Radial profiles of the plasma potentials and electron temperatures and densities were taken in the CASTOR tokamak edge plasma by cylindrical LPs perpendicular (shot #26402) and parallel (shot #27034) to the magnetic field lines and are presented in figures 13–16. The EEDFs were approximated by bi-Maxwellians with a high temperature part (indicated in figures by dots)

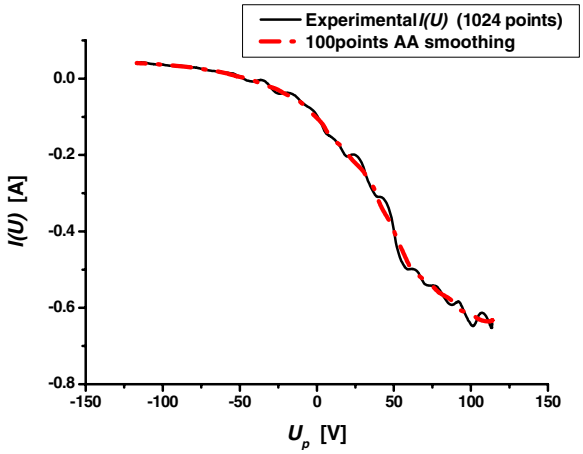

Figure 10. Single IV characteristic, shot #26402 for perpendicular probe #1 (solid line), on the steady-state phase of the plasma current ($10 < t < 11$ ms) and smoothed (dash–dot) by adjacent averaging of 100 points.

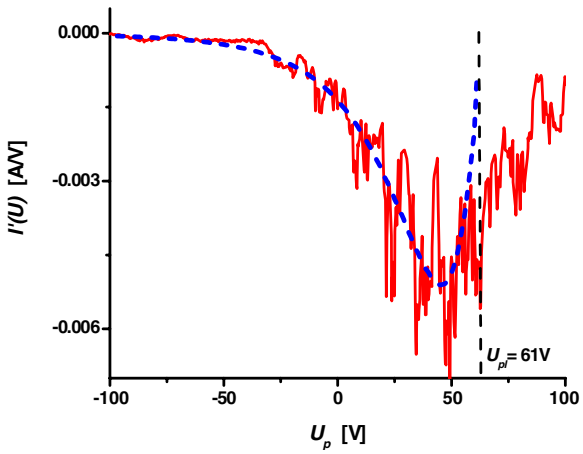

Figure 11. First derivative of the smoothed experimental IV curve, shot #26402 for perpendicular probe #1 (solid line). Model curve—dashed line.

and a low temperature part (triangles). The best fit with the experimental EEDF was sought with an accuracy of 15%. In the figures the positions of the last closed flux surface (LCFS) and the poloidal limiter are indicated. It should be noted that for perpendicular probes in the limiter shadow the EEDFs developed are mono-Maxwellian with a temperature of about 8 eV.

In the same figures the results obtained by the classic method [9] (squares) are also presented. We must point out that the classic method only assumes Maxwellian EEDF, which is in fact not representative of reality. The approximation for the probe current around the floating potential, $U_{\rm fl}$, and ion saturation current, $I_{\rm s}^i$, is

$$I(U) = I_{\rm s}^i \left\{ 1 - \exp\left[-\frac{e(U_{\rm fl} - U)}{T} \right] \right\}. \tag{22}$$

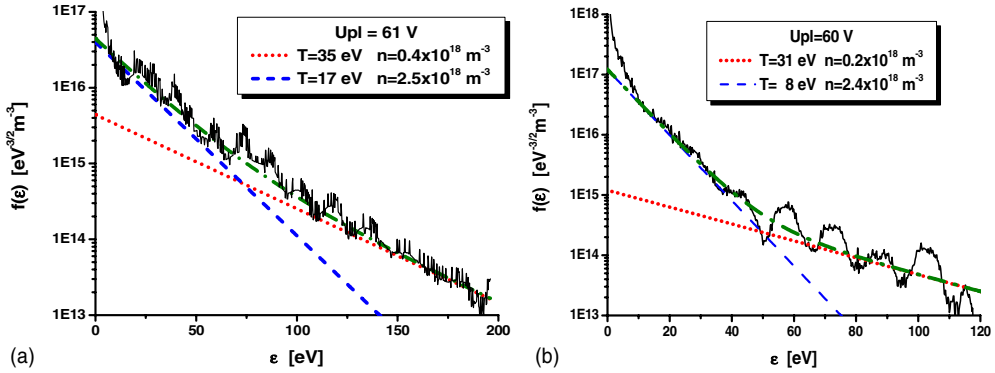

Figure 12. The EEDF obtained by (*a*) perpendicular probe #1, shot #26402 and (*b*) parallel probe #1, shot #27034 (black curves). The dash–dot line is bi-Maxwellian approximation. The dashed line represents the distribution of the low-energy electron population; the dotted line is the high energy one. The dash–dot line is a sum of the dotted line and the dashed line.

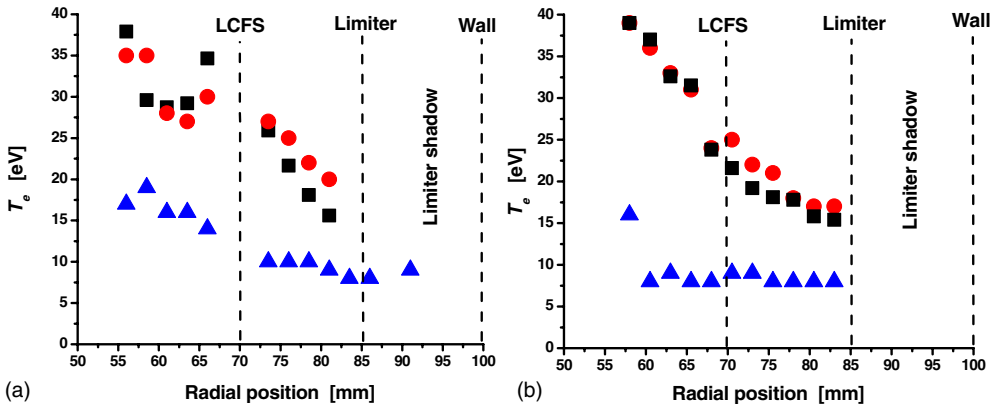

Figure 13. Electron temperatures at different radial positions as measured by (*a*) perpendicular oriented probes (shot #26402); (*b*) parallel oriented probes (shot #27034). The high temperatures are indicated by dots and the low temperatures by triangles. The results obtained with the classical method (squares) are also presented.

The IV probe characteristic around the floating potential (figure 14) is mostly affected by the high temperature electron fraction [11]. The low temperature electron fraction forms a part of the IV characteristic close to the plasma potential where the distortions due to the influence of the magnetic field are strongly pronounced. Thus the classic method is strongly affected by the fast electron temperature when the EEDF is bi-Maxwellian and as it is clearly seen from figure 12. We have good agreement between the measured data by the first derivative method and the classical one for the temperatures T of the minority high-energy electron fraction. The temperatures of the high-energy electron fraction measured by the first derivative probe method (figure 12(*a*)) and by the classical method (figure 14) are equal $T = 35$ eV. However, the classical method does not allow one to evaluate the temperature and the density of the predominant low-energy electron fraction of the bi-Maxwellian EEDF.

The classic approximation does not also allow the direct evaluation of the plasma potential. Using the first derivative probe method the radial distribution of the plasma potential was

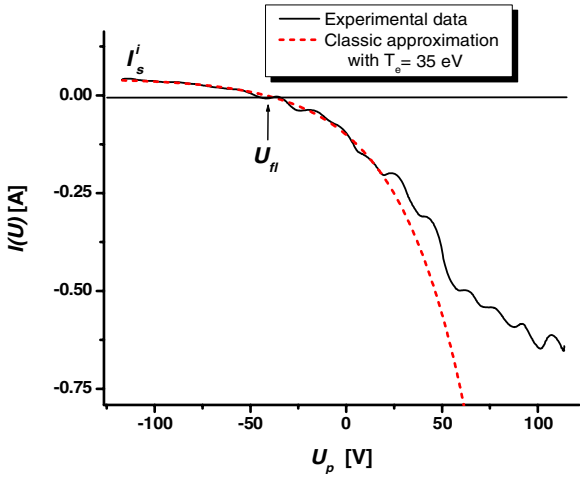

Figure 14. $I\,V$ from shot #26402; probe #1. Approximation with temperature $T = 35$ eV.

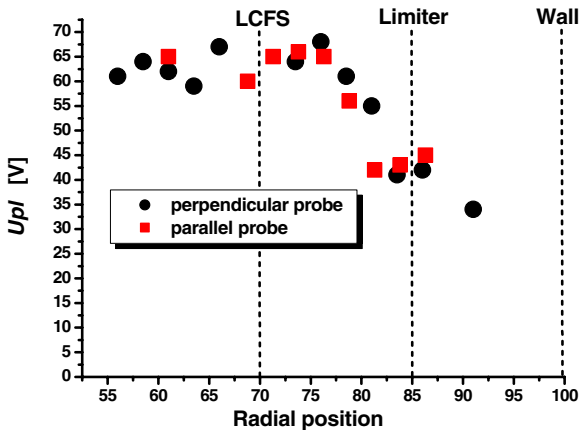

Figure 15. The radial distribution of the plasma potential for shot #26402 (dots) and shot #27034 (squares).

evaluated as it is presented in figure 15 for perpendicular probes (dots) and for parallel probes (squares). The accuracy of the evaluation is 20%.

The radial distribution of the total electron density, n, (dots) is presented for shot #26402 in figure 16(a) and for shot #27034 in figure 16(b). Triangles in the same figures represent the densities for high temperature electron fractions. They are in the range 0.2–0.4 $\times$ 10^{18} m^{-3} and are about 10% of the total electron densities. The uncertainty of the evaluations does not exceed 30%.

Comparison with the classical method (squares) is presented in figure 16. The total electron density was evaluated from the ion saturation current formula:

$$I_{\mathrm{s}}^{i} = 0.5 e n c_{\mathrm{s}} A_{\mathrm{p}}, \tag{23}$$

where A_{p} is the projection of the probe [26, 27] in the magnetic field $\vec{B}$ direction and $c_{\mathrm{s}} = [(T_{\mathrm{e}} + T_{\mathrm{i}})/m_{\mathrm{i}}]^{1/2}$ is the (isothermal) ion acoustic velocity [9]. We have to note that c_{s} is calculated with the electron temperature from the dense, 'cold' electron population and

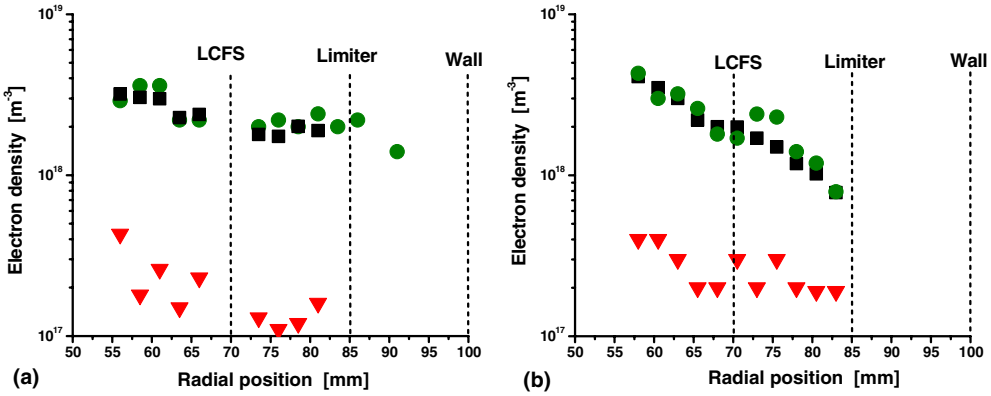

Figure 16. Radial distribution of the electron densities. The total electron densities are indicated by dots. The high temperature electron densities—by triangles. The results obtained by classical method (squares) are also presented, using the 'cold' electron population temperature. (*a*) Shot #26402 measurements by perpendicular probes; (*b*) shot #27034 measurements by parallel probes.

not using the one obtained by the approximation (22) giving the temperature of the less dense, 'hot' electron population. For the ion temperature, we assumed $T_i \approx T_e$. We observe good agreement with the total electron density obtained from the first derivative probe method.

Taking into account that the results presented in figures 13–16 are from different shots (see figure 8), the agreement between data processed by the first derivative method for parallel and perpendicular to the magnetic field probes is satisfactory.

5. Conclusion

The first derivative LP method for strongly magnetized plasmas is presented in this paper and was used for processing the electron part of the current–voltage characteristics measured in the CASTOR tokamak edge plasma. Measurements were carried out by cylindrical probes perpendicular and parallel to the magnetic field lines.

(1) Using the first derivative probe method the radial distribution of the plasma potential was evaluated.

(2) First results of the EEDFs at different radial positions for tokamak edge plasma are acquired. It is shown that in the edge plasma the EEDF is not Maxwellian but may be approximated by a bi-Maxwellian with a dominant cold electron population and a minority of hot electrons. In the limiter shadow the EEDFs developed is mono-Maxwellian.

(3) The values of the electron temperatures and density of the dominant cold electron population and the minority of hot electrons at different radial positions for tokamak edge plasma are evaluated.

The comparison of the results obtained with perpendicular and parallel to the magnetic field probes as well as the results given by the classic method leads to a satisfactory agreement.

The results presented demonstrate that the procedure proposed allows one to acquire additional plasma parameters using the electron part of the current–voltage LP characteristics in tokamak edge plasma measurements than in the classical method, which uses the ion part of the IV characteristic.

Acknowledgments

The authors wish to thank Dr B J Green for initiation of this work.

The results presented are in implementation of task P4 of Work Plan 2008 of the Association EURATOM/INRNE.BG in collaboration with the Association EURATOM/IPP.CR, Prague, Czech Republic.

References

[1] Druyvesteyn M J 1930 *Z. Phys.* **64** 781–98
[2] Kagan Y M and Perel V I 1964 *Sov. Phys.—Usp.* **6** 767
[3] Chen F F 1965 *Electric Probes Plasma Diagnostic Techniques* ed R H Huddlestone and S L Leonard (New York: Academic) chapter 4, pp 113–200
[4] Swift J D and Schwar M J R 1969 *Electrical Probes for Plasma Diagnostics* (New York: Elsevier)
[5] Hershkowitz N 1989 How Langmuir probes work *Plasma Diagnostics* vol 1, ed O Auciello and D L Flamm (Boston: Academic) chapter 3
[6] Demidov V I, Kolokolov N B and Kudryavtsev A A 1996 *Probe Methods for Low-Temperature Plasma Investigations* (Moscow: Energoatomizdat) (in Russian)
[7] Popov T K, Dimitrova M, Dias F M, Tsaneva V N, Stelmashenko N A, Blamire M G and Barber Z H 2006 *J. Phys. Conf. series* **44** 60–9
[8] Tagle J A, Stangeby P C and Erents S K 1987 *Plasma Phys. Control. Fusion* **29** 297–301
[9] Stangeby P C and McCracken G M 1990 *Nucl. Fusion* **30** 1225–38
[10] Fussmann G *et al* 1984 *J. Nucl. Mater.* **128 and 129** 350
[11] Stangeby P C 1995 *Plasma Phys. Control Fusion* **37** 1031–7
[12] Popov T K, Ivanova P, Stöckel J, Dejarnac R and Dias F M *34th EPS Conf. on Plasma Physics (Warsaw, Poland, 2–6 July 2007)* (ECA) vol 31F P5.104
[13] Gunn J P, Panek R, Stockel J, Van Oost G and Van Rompuy T 2005 *Czech. J. Phys.* **55** 255–63
[14] Van Rompuy T, Gunn J P, Dejarnac R, Stockel J and Van Oost G 2007 *Plasma Phys. Control. Fusion* **49** 619–29
[15] Van Rompuy T, Gunn J P and Van Oost G 2008 *Contrib. Plasma Phys.* **48** 497–502
[16] Golubovsky Yu B *et al* 1981 *Sov. J. Plasma Phys.* **7** 340
[17] Arslanbekov R R, Khromov N A and Kudryavtsev A A 1994 *Plasma Sources Sci. Technol.* **3** 528–38
[18] Golant V E, Zhilinski A P and Sakharov I E 1980 *Fundam. Plasma Phys.* (New York: Wiley)
[19] Martines E, Hron M and Stöckel J 2002*Plasma Phys. Control. Fusion* **44** 351
[20] Chen F F 1976 *Introduction to Plasma Physics* (New York: Plenum)
[21] Demidov V I, Ratynskaia S V, Armstrong R and Rypdal K 1999 *Phys. Plasma* **6** 350–8
[22] Demidov V I, Ratynskaia S V and Rypdal K 2002 *Rev. Sci. Instrum.* **73** 3409–39
[23] Popov T K, Ivanova P, Dimitrova M, Stöckel J and Dejarnac R 2008 *J. Phys. Conf. Ser.* **113** 012004
[24] Hidalgo C, Balbin R, Pedrosa M, Garcia Cortes I and Ochando M 1992 *Phys. Rev. Lett.* **69** 1205–08
[25] Popov T K, Ivanova P, Benova E, Bogdanov T, Dias F M, Stöckel J and Dejarnac R 2008 *35th EPS Conf. on Plasma Physics (Hersonissos, Crete, Greece, 9–13 June 2008)* (ECA) vol 32 P4-081
[26] Dejarnac R, Gunn J P, Stöckel J, Adamek J, Brotankova J and Ionita C 2007 *Plasma Phys. Control. Fusion* **49** 1791–808
[27] Stöckel J *et al* 2006 *J. Phys. Conf. Ser.* **63** 012001